Diabetes. Author manuscript; available in PMC 2017 January 12.

Published in final edited form as:

Diabetes. 2016 November ; 65(11): 3352–3361. doi:10.2337/db16-0564.

Salsalate (Salicylate) Uncouples Mitochondria, Improves Glucose Homeostasis, and Reduces Liver Lipids Independent of AMPK-β1

Brennan K. Smith[1], **Rebecca J. Ford**[1], **Eric M. Desjardins**[1], **Alex E. Green**[1], **Meghan C. Hughes**[2], **Vanessa P. Houde**[1], **Emily A. Day**[1], **Katarina Marcinko**[1], **Justin D. Crane**[1], **Emilio P. Mottillo**[1], **Christopher G.R. Perry**[2], **Bruce E. Kemp**[3,4], **Mark A. Tarnopolsky**[5], and **Gregory R. Steinberg**[1,6]

[1]Division of Endocrinology and Metabolism, Department of Medicine, McMaster University, Hamilton, Ontario, Canada

[2]Muscle Health Research Centre, School of Kinesiology and Health Science, York University, Toronto, Ontario, Canada

[3]Protein Chemistry and Metabolism, St Vincent's Institute and Department of Medicine, University of Melbourne, Melbourne, Victoria, Australia

[4]Mary MacKillop Institute for Health Research, Australian Catholic University, Fitzroy, Victoria, Australia

[5]Department of Pediatrics, McMaster University, Hamilton, Ontario, Canada

[6]Department of Biochemistry and Biomedical Sciences, McMaster University, Hamilton, Ontario, Canada

Abstract

Salsalate is a prodrug of salicylate that lowers blood glucose in patients with type 2 diabetes (T2D) and reduces nonalcoholic fatty liver disease (NAFLD) in animal models; however, the mechanism mediating these effects is unclear. Salicylate directly activates AMPK via the β1 subunit, but whether salsalate requires AMPK-β1 to improve T2D and NAFLD has not been examined. Therefore, wild-type (WT) and AMPK-β1–knockout (AMPK-β1KO) mice were treated with a salsalate dose resulting in clinically relevant serum salicylate concentrations (~1 mmol/L). Salsalate treatment increased VO_2, lowered fasting glucose, improved glucose tolerance, and led to an ~55% reduction in liver lipid content. These effects were observed in both WT and AMPK-β1KO mice. To explain these AMPK-independent effects, we found that salicylate increases oligomycin-insensitive respiration (state 4o) and directly increases mitochondrial proton

Corresponding author: Gregory R. Steinberg, gsteinberg@mcmaster.ca.

Duality of Interest. No potential conflicts of interest relevant to this article were reported.

Author Contributions. B.K.S. and G.R.S. designed research studies, analyzed data, and wrote the manuscript. B.K.S., R.J.F., E.M.D., A.E.G., M.C.H., V.P.H., E.A.D., K.M., J.D.C., E.P.M., and C.G.R.P. conducted experiments and analyzed data. B.K.S., R.J.F., E.M.D., A.E.G., V.P.H., E.A.D., K.M., J.D.C., E.P.M., B.E.K., M.A.T., and G.R.S. edited the manuscript. G.R.S. is the guarantor of this work and, as such, had full access to all the data in the study and takes responsibility for the integrity of the data and the accuracy of the data analysis.

This article contains Supplementary Data online at http://diabetes.diabetesjournals.org/lookup/suppl/doi:10.2337/db16-0564/-/DC1.

conductance at clinical concentrations. This uncoupling effect is tightly correlated with the suppression of de novo lipogenesis. Salicylate is also able to stimulate brown adipose tissue respiration independent of uncoupling protein 1. These data indicate that the primary mechanism by which salsalate improves glucose homeostasis and NAFLD is via salicylate-driven mitochondrial uncoupling.

Nonalcoholic fatty liver disease (NAFLD) is considered an important contributing factor to the development of insulin resistance and type 2 diabetes (T2D) (1). Despite the rising prevalence of NAFLD and importance for the development of T2D, there are currently no pharmacological approaches for the treatment of this disease (2).

Salsalate is a prodrug of salicylate and is hydrolyzed in the small intestine to produce two molecules of salicylate (3,4). The circulating concentration of salicylate in humans administered salsalate in T2D clinical trials is ~1 mmol/L (5–8). Salsalate has also been shown to improve symptoms of NAFLD (9) and nonalcoholic steatohepatitis in mice (10). The mechanism by which salsalate improves T2D and NAFLD is currently unclear, although multiple mechanisms have been proposed (10–16). The mechanism of action most commonly associated with salsalate is the direct repressing effect of salicylate on inhibitor of nuclear factor κ-B kinase subunit β (IKK-β) to reduce inflammation (11–13). However, the concentration of salicylate used in these studies nonspecifically inhibits many protein kinases through direct competition with their ATP binding sites (16–18). In contrast to kinase inhibition, salicylate has also been shown to directly activate AMPK, a metabolic-sensing enzyme important for regulating inflammation (19), liver lipid metabolism (20), and brown fat thermogenesis (21,22). The effect of salicylate on AMPK occurs via a direct interaction with the Ser108 residue of the β1 subunit (16,23). The most recent proposal to explain the mechanism of salicylate suggests that salsalate can activate brown adipose tissue (BAT) through activation of cAMP-dependent protein kinase (15).

Although salicylate directly activates AMPK via the β1 subunit, daily intraperitoneal injections of salicylate (250 mg/kg) improved a marker of HOMA insulin resistance in both wild-type (WT) and AMPK-β1–knockout (KO) mice fed a high-fat diet (HFD) (16). Because the dose of salicylate used in this study results in serum concentrations of salicylate more than double the clinical levels after the oral intake of salsalate (~2.4 mmol/L compared with ~1.0 mmol/L, respectively) we hypothesized that the AMPK-β1–independent effects may have been a result of off-target kinase inhibition (16–18).

The purpose of this study was to investigate whether oral delivery of clinically relevant concentrations of salsa-late improves glucose homeostasis and reduces NAFLD through an AMPK-β1–dependent pathway. Salsalate was observed to improve whole-body glucose homeostasis, reduce liver lipid content, and improve adipose tissue inflammation independently of AMPK-β1. These diverse metabolic effects of salsalate are associated with the protonophoric effects of salicylate and subsequent mitochondrial uncoupling and increased energy expenditure. These data suggest that salicylate-driven mitochondrial uncoupling is the primary mechanism mediating the beneficial effects of salsalate therapy on NAFLD and T2D.

RESEARCH DESIGN AND METHODS

Study Approval

All animal procedures were approved by the McMaster University Animal Ethics Research Board (AUP #: 12-12-44; Hamilton, Ontario, Canada) and conform to the *Guide for the Care and Use of Laboratory Animals* published by the U.S. National Institutes of Health.

Animals

WT and AMPK-β1KO mice were started on an HFD (60% calories from fat) at 8 weeks of age. At 4 weeks after the initiation of the HFD, half of the mice continued on the HFD and the other half were switched to an HFD supplemented with 2.5 g/kg salsalate. These diets were maintained for 8 weeks until sacrifice (Supplementary Fig. 1*A*). The glucose tolerance test was performed in 6-h fasted mice after an injection of glucose (0.8 g/kg i.p.). The alanine tolerance test was performed in 16-h fasted mice after an injection of alanine (2 g/kg i.p.) (24). Blood glucose levels were determined from a small tail vein nick using a One Touch Ultra Glucometer (LifeScan Canada). Metabolic monitoring was performed in a Comprehensive Lab Animal Monitoring System (CLAMS), an indirect calorimetry system (Columbus Instruments, Columbus, OH) at week 10. Nonmoving VO_2 measurements were taken under light anesthetic to remove activity level confounding (25,26). To assess uncoupling protein 1 (UCP1)–mediated thermogenesis, CL-316,243 (0.033 nmol/g body weight) administration was performed as previously described (26). In a subset of animals, insulin (1 unit/kg) was administered before sacrifice to examine insulin signaling in the liver and 2-deoxy-D-glucose uptake into skeletal muscle and adipose tissue (27).

Analytical Measurements

Serum salicylate concentrations were determined from a commercially available kit (Neogen Corporation) following the manufacturer's instructions. Liver sections were stained with hematoxylin and eosin. Liver and tibialis anterior samples were extracted by the Folch method to measure tissue triglyceride levels (28). Primary hepatocytes were freshly isolated by collagenase perfusion for the lipogenesis and respiration measurements. Mitochondrial membrane potential ($\Delta\psi m$) was measured using the tetramethyl rhodamine methyl ester (TMRM) stain (20 nmol/L, nonquenching) (29). Primary hepatocyte de novo lipogenesis was measured similar to previous reports using ^3H acetate (PerkinElmer) (20). Quantitative real-time PCR was performed as previously described to determine mRNA expression levels (19). Briefly, epididymal adipose tissue was lysed in TRIzol reagent (Invitrogen, Carlsbad, CA) to remove lipid, and the aqueous phase was applied to an RNeasy kit (Qiagen, Valencia, CA) column for subsequent purification. Relative gene expression was calculated using the comparative Ct ($2^{-\Delta\Delta Ct}$) method, where values were normalized to the housekeeping gene *Ppia*. TaqMan primers F4/80 (*Emr1*, Mm00802529_m1), cluster of differentiation 68 (*Cd68,* Mm00839636_g1), tumor necrosis factor-α (*Tnf-α*, Mm00443258_m1), chemokine (C-C motif) ligand 2 (*CCL2*, Mm00441242_m1), and interleukin-1β (*Il-1β*, Mm00434228_m1), were purchased from Invitrogen. Western blotting was performed similar to the description by Ford et al. (9), and all antibodies were purchased from Cell Signaling. ATP concentration was determined in freeze-clamped liver tissue according to the manufacturer's instruction (ab113849; Abcam) (30).

Respiration Methods

Mitochondrial respiration was measured by high-resolution respirometry (Oxygraph-2k; Oroboros, Innsbruck, Austria) at 37°C and room air saturated oxygen tension. Permeabilized primary hepatocyte respiration was performed in MIRO5 buffer containing EGTA (0.5 mmol/L), $MgCl_2$*$6H_2O$ (3 mmol/L), K-lactobionate (60 mmol/L), KH_2PO_4 (10 mmol/L), HEPES (20 mmol/L), sucrose (110 mmol/L), and fatty acid–free BSA (1 g/L). Primary hepatocytes were scraped into 2 mL of respiration buffer, and 800 µL of the suspension was quickly added to the respiration chambers. Digitonin (8.1 µmol/L) was added to the chambers to permeabilize the cells, and the assay was initiated after a 5-min incubation period. Permeabilized skeletal muscle fibers and epididymal adipose tissue were prepared as previously described (31,32). BAT mitochondria were isolated, and respiration was performed similar to previous reports (33,34).

Mitochondrial Proton Conductance

Isolated liver mitochondrial VO_2 rates and $\Delta\psi m$ were measured simultaneously in the Oroboros system at 37°C (35,36). Mitochondria were isolated similar to previous descriptions (37), and experiments were run in Buffer Z containing K-2-(N-morpholino)ethanesulfonic acid (110 mmol/L), KCl (35 mmol/L), EGTA (1 mmol/L), K_2HPO_4 (5 mmol/L), $MgCl_2$*$6H_2O$ (3 mmol/L), and BSA (0.5 mg/mL), pH 7.1, 295 mOsm. Buffer Z was supplemented with carboxy atractyloside (1.5 µmol/L), oligomycin (1.25 µg/mL), guanosine diphosphate (GDP) (0.5 mmol/L), nigericin (0.1 µmol/L), rotenone (5 µmol/L), and succinate (6 mmol/L). $\Delta\psi m$ was measured using electrodes sensitive to tetraphenylphosponium (TPP^+), and the TPP^+ electrode was calibrated by a 5-point titration (0.9–1.7 µmol/L, every 2 µmol/L) at the beginning of each experiment. $\Delta\psi m$ was lowered by titration of the complex II inhibitor malonate (0.1 to 5 mmol/L) in the absence or presence of 1 mmol/L salicylate. Salicylate was also titrated directly into respiration chambers.

Acute Effects of Salsalate In Vivo

To assess the acute effects of salsalate on in vivo lipogenesis, energy expenditure, VO_2, and VCO_2, mice were intraperitoneally injected with salsalate (Cayman Chemicals) or vehicle. Salsalate was initially dissolved in 100% DMSO and then further suspended in 20% 2-hydroxypropyl-β-cyclodextrin (Sigma-Aldrich) in saline down to a final concentration of 5% DMSO. The vehicle control for these experiments was the same stock of 20% 2-hydroxypropyl-β-cyclodextrin (in saline) with 5% DMSO. In vivo lipogenesis was performed similar to previous reports (20,38). Mice were fasted for 15 h, refed for 2 h, and then 20 µCi of ^3H acetate (PerkinElmer) was intraperitoneally injected into the mouse. The mice were intraperitoneally injected 15 min later with salsalate or vehicle made up as above. The mice were sacrificed 1 h later (Supplementary Fig. 1*B*).

The lipids were extracted by the Folch method, and the entire chloroform layer was counted for radioactivity. The liver was also examined for measurements of AMPK activation and ATP concentration. For acute changes in energy expenditure, 1 h after the administration of salsalate or vehicle, mice were lightly anesthetized with an intraperitoneal injection of 0.5 mg/g body weight Avertin (2,2,2-tribromoethanol dissolved in 2-methyl-2-butanol; Sigma-

Aldrich) to obtain nonmoving measurements. This protocol was undertaken to ensure that energy expenditure associated with activity (skeletal muscle contraction) would not confound our energy expenditure data. The mice were placed dorsal side up onto an enclosed stationary treadmill and metabolic measurements were monitored for 12 min using CLAMS (Supplementary Fig. 1*C*).

Statistical Analyses

Values are reported as mean ± SEM. Data were analyzed using two-way or one-way ANOVA with Bonferroni post hoc test or Student *t* test where indicated. Differences were considered significant when $P < 0.05$.

RESULTS

Salsalate Treatment Improves Glucose Homeostasis and Reduces Liver Lipids Independent of AMPK-β1

Salsalate (2.5 g/kg) supplemented in a 60% HFD gave serum salicylate values of ~800–900 μmol/L (Fig. 1*A*) matching clinical levels (5). WT and AMPK-β1KO mice were fed the HFD for 4 weeks, followed by 8 weeks of the HFD or HFD with salsalate supplementation. Significant differences in body mass were not observed (Fig. 1*B*), but salsalate supplementation significantly reduced the percentage of adiposity and increased the percentage of lean mass (Fig. 1*C* and *D*). An increase in nonmoving VO_2 was observed (Fig. 1*E*), although examination of the mice in the free-living state indicated no differences in VO_2, energy expenditure, VCO_2, activity levels, or food intake (Supplementary Fig. 2).

Fasting glucose levels and glucose tolerance were improved by salsalate in both WT and AMPK-β1KO mice (Fig. 1*F*–*H*). Salsalate supplementation improved alanine tolerance (Fig. 1*I* and *J*), suggesting reductions in hepatic gluconeogenesis. Reductions in liver lipid content in WT and AMPK-β1KO mice were also observed (Fig. 1*K* and *L*). Lipid levels in the tibialis anterior muscle were not significantly reduced by salsalate (Supplementary Fig. 3). Consistent with reductions in adiposity in both WT and AMPK-β1KO mice (Fig. 1*C*), markers of adipose tissue inflammation were generally reduced in both genotypes after treatment with salsalate (Supplementary Fig. 4). Insulin-stimulated 2-deoxy-D-glucose uptake into skeletal muscle (Supplementary Fig. 5*A*) and inguinal white adipose tissue (Supplementary Fig. 5*B*) was not different between genotypes or after salsalate treatment. Liver AKT phosphorylation at Thr308 and insulin receptor substrate 1 phosphorylation at Tyr1222 were also unchanged (Supplementary Fig. 6). Therefore, a clinically relevant dose of salsalate increases nonmoving VO_2, improves glucose homeostasis, lowers markers of adipose tissue inflammation, and reduces liver lipids independent of AMPK-β1.

Salicylate Uncouples Mitochondria

To explore AMPK-β1–independent mechanisms by which salsalate may increase VO_2, reduce liver lipid content, and improve glucose homeostasis, the ability of salicylate to uncouple mitochondria at clinical concentrations in permeabilized primary hepatocytes was examined. To this end, permeabilized primary hepatocyte respiration was stimulated with glutamate, malate, and ADP to induce state 3 respiration, and in a stepwise fashion the

following were added: *1*) cytochrome *c* to check for outer mitochondrial membrane integrity (39), *2*) GDP to inhibit uncoupling proteins (40,41), *3*) oligomycin to inhibit ATP synthase (42), and *4*) salicylate at increasing concentrations. Salicylate increases respiration independent of uncoupling proteins and ATP synthase in a dose-dependent manner at concentrations starting as low as 0.1 mmol/L in WT (Fig. 2*A* and *B*) and AMPK-β1KO hepatocytes (Supplementary Fig. 7*A*). Similar observations were also observed in permeabilized skeletal muscle fibers (Supplementary Fig. 7*B*) and epididymal white adipose tissue (Supplementary Fig. 7*C*).

To further examine the concept of mitochondrial uncoupling, Δψm was measured using TMRM staining, and salicylate was observed to dose-dependently decrease Δψm (Fig. 2*C* and *D*). Mitochondrial proton conductance assays were then performed, and in the presence of 1.0 mmol/L salicylate, proton current was elevated at a given membrane potential (Fig. 2*E*). Salicylate also directly increased mitochondrial proton conductance (Fig. 2*F*). Thus, the protonophoric effect of salicylate can explain the salicylate-induced mitochondrial uncoupling, the increase in VO_2 in vitro and in vivo, and the AMPK-β1–independent effects of salsalate.

Subclinical Salicylate Treatment Suppresses Primary Hepatocyte De Novo Lipogenesis

The mechanism by which mitochondrial uncoupling is traditionally viewed to improve metabolic health is associated with increases in substrate oxidation; however, the suppression of anabolism may also play a role. Indeed, human subjects with NAFLD display a fivefold increase in rates of fatty acid synthesis (de novo lipogenesis [DNL]) (43,44). Therefore, the effects of clinical salicylate concentrations on DNL were examined and correlated with mitochondrial uncoupling.

Salicylate dose-dependently suppressed primary hepatocyte DNL at subclinical concentrations (Fig. 3*A*), and this suppression in DNL correlated with the salicylate-driven increases in uncoupled respiration (Fig. 3*B* and *C*). In addition, when hepatocytes were treated with two classic mitochondrial uncouplers, 2,4 dinitrophenol (DNP) and carbonyl cyanide-4-(trifluoromethoxy) phenylhydrazone, DNL rates were significantly reduced (Fig. 3*D*). These data highlight the importance of Δψm in the maintenance of DNL.

To investigate a role for AMPK in mediating the DNL-lowering effects of salicylate, DNL rates were examined in AMPK-β1KO primary hepatocytes. AMPK is also known to inhibit DNL via phosphorylation of Ser79/212 on acetyl-CoA carboxylase (ACC) (45), and so the effects of salicylate in a double-knockin (ACC-DKI) model harboring serine to alanine mutations on these two residues were analyzed (20). DNL rates were inhibited by salicylate in primary hepatocytes derived from AMPK-β1KO and ACC-DKI mice, indicating that salicylate inhibits DNL independent of AMPK-β1 and AMPK-ACC signaling (Fig. 3*E*).

Salsalate Suppresses Liver De Novo Lipogenesis In Vivo

To investigate whether these in vitro effects regarding DNL occurred in vivo, an acute salsalate dose that gives rise to circulating salicylate concentrations similar to human clinical data and the in vivo feeding study was examined. An acute injection of salsalate (62.5 mg/kg i.p.) in mice resulted in clinically relevant serum concentrations of salicylate (Fig. 4*A*). This

dose is equivalent to a 70-kg human ingesting 4.2 g of salsalate, which is aligned with clinical dosing (3.5–4.5 g) (5,7). After an acute treatment with salsalate (62.5 mg/kg), nonmoving VO_2, VCO_2, and energy expenditure were increased, effects that are characteristic of mitochondrial uncoupling (Fig. 4*B–D*, method outlined in Supplementary Fig. 1*C*). In addition, salsalate reduced in vivo DNL rates by ~25% (Fig. 4*E*, method outlined in Supplementary Fig. 1*B*), and these effects were independent of changes in AMPK activation or ATP levels (Supplementary Fig. 8). Collectively, these data suggest that salsalate, via salicylate-driven mitochondrial uncoupling, increases energy expenditure and suppresses DNL in vivo.

Salicylate Increases Respiration in BAT Mitochondria Independent of UCP1

BAT activation increases energy expenditure, and strategies to increase BAT activation have shown therapeutic promise for treating NAFLD and T2D (46,47), effects that largely depend on the activation of UCP1 (48).

A recent study showed that salsalate directly activates BAT to increase energy expenditure and improve HFD-induced metabolic dysfunction (15). To further examine this proposed mechanism of action, salsalate-treated mice were analyzed using an in vivo technique that specifically detects UCP1-mediated thermogenesis (26). Upon analysis, salsalate treatment did not alter UCP1-mediated thermogenesis in response to β3 adrenergic stimulation in vivo (Fig. 5*A–D*), suggesting salsalate-induced increases in whole body VO_2 does not depend on increases in UCP1 activation. Therefore, UCP1-independent BAT mitochondrial activity was investigated in response to salicylate. To this end, BAT mitochondria were isolated, and respiration was stimulated with palmitoyl-CoA (30 μmol/L) and then inhibited with the UCP1 inhibitor GDP (2 mmol/L) (34). Salicylate dose dependently increased VO_2 even when UCP1 was inhibited by GDP (Fig. 5*E* and *F*). These data indicate that salicylate increases BAT mitochondrial VO_2 independent of UCP1.

DISCUSSION

Various mechanisms have been proposed to explain the beneficial health effects associated with salsalate/salicylate. This is the first study to suggest that salicylate-driven mitochondrial uncoupling is the primary mechanism of action to explain the host of beneficial effects associated with salicylate (11,49,50) and salsalate (6–8,14,51,52). Data from the present study and previous investigations suggest that mitochondrial uncoupling resulting from the protonophoric properties of salicylate explains the consistently observed increases in energy expenditure in murine models and human subjects treated with salicylate-based compounds (6,10,11,14,15,52–58).

Classic studies from the 1950s observed that salicylate stimulates mitochondrial uncoupling (53,59), and previous work established that mitochondrial $\Delta\psi m$ is reduced by 1.0 mmol/L salicylate (54). Moreover, proton conductance is increased with 1.0 mmol/L salicylate treatment (present data and ref. 54), and these bioenergetic effects are likely due to the ability of salicylate to act as a proton carrier (60,61). The current study extends this bioenergetic mechanism of salicylate into the regulation of whole-body physiology.

From a therapeutic perspective, the beneficial effects of mitochondrial protonophores (uncouplers) on T2D and NAFLD have been consistently observed (62–66). The compounds recently studied include a modified version of the classic protonophore, DNP (62), which is structurally similar to salicylate (53,67). These mitochondrial uncouplers result in an increase in energy expenditure similar to that obtained when treating with salsalate/salicylate (present work and previous studies [6,10,11,14,15,52–58]) and also improve markers of NAFLD and T2D (62–66). Therefore, considering that mitochondrial uncouplers improve T2D and NAFLD, and increasing energy expenditure is a potent mechanism to improve T2D and NAFLD (62,63,68–70), the present work, together with previous reports in mice and humans, is highly suggestive that salicylate-driven mitochondrial uncoupling is the primary mechanism of action explaining the improvement in T2D and NAFLD associated with salsalate treatment.

As a potential mechanism to explain why mitochondrial uncouplers improve T2D and NAFLD, salsalate was found to potently suppress hepatic DNL in vitro and in vivo. NAFLD is associated with increased rates of hepatic DNL (43,44), and this report is the first to show that DNL can be suppressed in vivo with an acute, therapeutically relevant dose of salsalate. DNL requires three basic constituents; substrate (acetyl-CoA), reductive power (NADPH), and energy supply (ATP). By reducing $\Delta\psi m$, salicylate and other uncoupling agents compromise the availability of all three factors as the cell shifts to a catabolic state and downregulates anabolic activity (67,71). Considering the potential importance of DNL in human NAFLD, future work investigating whether salsalate can suppress DNL in humans is warranted.

From a general mechanism standpoint, previous work in humans supplemented with high-dose aspirin (57) or salsalate (14) observed increases in carbohydrate and fat oxidation. The only way carbohydrate and fat oxidation can simultaneously increase in vivo is if the overall demand of the system (i.e., uncoupling or increased ATP turnover) changes. In the case of salsalate, by providing a protonophore (salicylate), $\Delta\psi m$ is reduced, an effect that allows fat and carbohydrate catabolism to increase. In environments typified by overnutrition, this uncoupling mechanism works to blunt the toxic excess of substrate by siphoning fat and/or carbohydrate away from anabolic pathways (DNL) in favor of oxidation. In other words, mitochondrial uncouplers suppress the toxic effects of substrate oversupply by removing the substrate.

A limitation of this work is that definitive genetic evidence is unavailable because removing mitochondria and, therefore, the uncoupling effects of salicylate, is not possible. A further limitation is the difficulty in discerning which cell type or organ system is playing the most prominent role in mediating the beneficial effects of salsalate. Inhibition of hepatic DNL has shown therapeutic promise for NAFLD (72), as has promoting hepatic substrate consumption (62), indicating that the liver may be important. However, increasing BAT mitochondrial activity has been shown to spare the liver from substrate oversupply (46), and skeletal muscle is responsible for the majority of glucose clearance (73). Further work is thus required to investigate which organ system is playing the most prominent role.

In addition to the positive metabolic effects associated with mitochondrial uncouplers in the presence of nutrient excess, significant negative adverse effects have been associated with uncoupling agents, including DNP (74,75). The present report is an important message from not only a therapeutic perspective but also from a potential adverse effects perspective, and future work examining salicylate-based compounds should consider the fact that salicylate uncouples mitochondria at clinically relevant concentrations.

In summary, a therapeutically relevant dose of salsalate improves glucose homeostasis, lowers adipose tissue inflammation, and reduces liver lipid content, independent of AMPK-β1. Instead of AMPK, it seems likely that the protonophoric effect of salicylate is the primary mechanism underlying the metabolic improvements associated with salicylate (11,49) and salsalate (6–8,14,51,52) under conditions of nutrient excess. Future studies should consider this mechanism of action when examining effects of salsalate on T2D and NAFLD.

Supplementary Material

Refer to Web version on PubMed Central for supplementary material.

Acknowledgments

Funding. B.K.S. is a recipient of a Canadian Institutes of Health Research (CIHR) Postdoctoral Fellowship and Michael G. DeGroote Postdoctoral Fellowship. E.M.D. is a recipient of an Ontario Graduate Scholarship and Queen Elizabeth II Graduate Scholarship in Science and Technology. A.E.G. is a recipient of a Canadian Graduate Scholarship from CIHR/MitoCanada. E.P.M. is a Canadian Diabetes Association postdoctoral fellow. B.E.K. is supported by grants and a fellowship from the Australian Research Council and the National Health and Medical Research Council, supported in part by the Victorian Government's Operational Infrastructure. These studies were supported by grants from the Canadian Diabetes Association (G.R.S.), the CIHR (G.R.S.), and the Natural Sciences and Engineering Research Council of Canada (G.R.S.). G.R.S. is a Canada Research Chair in Metabolism and Obesity and the J. Bruce Duncan Chair in Metabolic Diseases.

References

1. Rinella ME. Nonalcoholic fatty liver disease: a systematic review. JAMA. 2015; 313:2263–2273. [PubMed: 26057287]
2. Perry RJ, Samuel VT, Petersen KF, Shulman GI. The role of hepatic lipids in hepatic insulin resistance and type 2 diabetes. Nature. 2014; 510:84–91. [PubMed: 24899308]
3. Dromgoole SH, Cassell S, Furst DE, Paulus HE. Availability of salicylate from salsalate and aspirin. Clin Pharmacol Ther. 1983; 34:539–545. [PubMed: 6617077]
4. Dromgoole SH, Furst DE, Paulus HE. Metabolism of salsalate in normal subjects. J Pharm Sci. 1984; 73:1657–1659. [PubMed: 6520777]
5. Fleischman A, Shoelson SE, Bernier R, Goldfine AB. Salsalate improves glycemia and inflammatory parameters in obese young adults. Diabetes Care. 2008; 31:289–294. [PubMed: 17959861]
6. Goldfine AB, Silver R, Aldhahi W, et al. Use of salsalate to target inflammation in the treatment of insulin resistance and type 2 diabetes. Clin Transl Sci. 2008; 1:36–43. [PubMed: 19337387]
7. Goldfine AB, Fonseca V, Jablonski KA, Pyle L, Staten MA, Shoelson SE. TINSAL-T2D (Targeting Inflammation Using Salsalate in Type 2 Diabetes) Study Team. The effects of salsalate on glycemic control in patients with type 2 diabetes: a randomized trial. Ann Intern Med. 2010; 152:346–357. [PubMed: 20231565]
8. Barzilay JI, Jablonski KA, Fonseca V, et al. TINSAL-T2D Research Consortium. The impact of salsalate treatment on serum levels of advanced glycation end products in type 2 diabetes. Diabetes Care. 2014; 37:1083–1091. [PubMed: 24255104]

9. Ford RJ, Fullerton MD, Pinkosky SL, et al. Metformin and salicylate synergistically activate liver AMPK, inhibit lipogenesis and improve insulin sensitivity. Biochem J. 2015; 468:125–132. [PubMed: 25742316]
10. Liang W, Verschuren L, Mulder P, et al. Salsalate attenuates diet induced non-alcoholic steatohepatitis in mice by decreasing lipogenic and inflammatory processes. Br J Pharmacol. 2015; 172:5293–5305. [PubMed: 26292849]
11. Kim JK, Kim YJ, Fillmore JJ, et al. Prevention of fat-induced insulin resistance by salicylate. J Clin Invest. 2001; 108:437–446. [PubMed: 11489937]
12. Yuan M, Konstantopoulos N, Lee J, et al. Reversal of obesity- and diet-induced insulin resistance with salicylates or targeted disruption of Ikkbeta. Science. 2001; 293:1673–1677. [PubMed: 11533494]
13. Yin MJ, Yamamoto Y, Gaynor RB. The anti-inflammatory agents aspirin and salicylate inhibit the activity of I(kappa)B kinase-beta. Nature. 1998; 396:77–80. [PubMed: 9817203]
14. Meex RC, Phielix E, Moonen-Kornips E, Schrauwen P, Hesselink MK. Stimulation of human whole-body energy expenditure by salsalate is fueled by higher lipid oxidation under fasting conditions and by higher oxidative glucose disposal under insulin-stimulated conditions. J Clin Endocrinol Metab. 2011; 96:1415–1423. [PubMed: 21289240]
15. van Dam AD, Nahon KJ, Kooijman S, et al. Salsalate activates brown adipose tissue in mice. Diabetes. 2015; 64:1544–1554. [PubMed: 25475439]
16. Hawley SA, Fullerton MD, Ross FA, et al. The ancient drug salicylate directly activates AMP-activated protein kinase. Science. 2012; 336:918–922. [PubMed: 22517326]
17. Alpert D, Vilcek J. Inhibition of IkappaB kinase activity by sodium salicylate in vitro does not reflect its inhibitory mechanism in intact cells. J Biol Chem. 2000; 275:10925–10929. [PubMed: 10753891]
18. Steinberg GR, Dandapani M, Hardie DG. AMPK: mediating the metabolic effects of salicylate-based drugs? Trends Endocrinol Metab. 2013; 24:481–487. [PubMed: 23871515]
19. Galic S, Fullerton MD, Schertzer JD, et al. Hematopoietic AMPK β1 reduces mouse adipose tissue macrophage inflammation and insulin resistance in obesity. J Clin Invest. 2011; 121:4903–4915. [PubMed: 22080866]
20. Fullerton MD, Galic S, Marcinko K, et al. Single phosphorylation sites in Acc1 and Acc2 regulate lipid homeostasis and the insulin-sensitizing effects of metformin. Nat Med. 2013; 19:1649–1654. [PubMed: 24185692]
21. Mottillo EP, Desjardins EM, Crane JD, et al. Lack of adipocyte AMPK exacerbates insulin resistance and hepatic steatosis through brown and beige adipose tissue function. Cell Metab. 2016; 24:118–129. [PubMed: 27411013]
22. Zhang H, Guan M, Townsend KL, et al. MicroRNA-455 regulates brown adipogenesis via a novel HIF1an-AMPK-PGC1α signaling network. EMBO Rep. 2015; 16:1378–1393. [PubMed: 26303948]
23. Calabrese MF, Rajamohan F, Harris MS, et al. Structural basis for AMPK activation: natural and synthetic ligands regulate kinase activity from opposite poles by different molecular mechanisms. Structure. 2014; 22:1161–1172. [PubMed: 25066137]
24. Bujak AL, Crane JD, Lally JS, et al. AMPK activation of muscle autophagy prevents fasting-induced hypoglycemia and myopathy during aging. Cell Metab. 2015; 21:883–890. [PubMed: 26039451]
25. O'Neill HM, Maarbjerg SJ, Crane JD, et al. AMP-activated protein kinase (AMPK) beta1beta2 muscle null mice reveal an essential role for AMPK in maintaining mitochondrial content and glucose uptake during exercise. Proc Natl Acad Sci U S A. 2011; 108:16092–16097. [PubMed: 21896769]
26. Crane JD, Mottillo EP, Farncombe TH, Morrison KM, Steinberg GR. A standardized infrared imaging technique that specifically detects UCP1-mediated thermogenesis in vivo. Mol Metab. 2014; 3:490–494. [PubMed: 24944909]
27. Howlett KF, Andrikopoulos S, Proietto J, Hargreaves M. Exercise-induced muscle glucose uptake in mice with graded, muscle-specific GLUT-4 deletion. Physiol Rep. 2013; 1:e00065. [PubMed: 24303141]

28. Folch J, Lees M, Sloane Stanley GH. A simple method for the isolation and purification of total lipides from animal tissues. J Biol Chem. 1957; 226:497–509. [PubMed: 13428781]
29. Scaduto RC Jr, Grotyohann LW. Measurement of mitochondrial membrane potential using fluorescent rhodamine derivatives. Biophys J. 1999; 76:469–477. [PubMed: 9876159]
30. Borowski LS, Dziembowski A, Hejnowicz MS, Stepien PP, Szczesny RJ. Human mitochondrial RNA decay mediated by PNPase-hSuv3 complex takes place in distinct foci. Nucleic Acids Res. 2013; 41:1223–1240. [PubMed: 23221631]
31. Smith BK, Perry CG, Herbst EA, et al. Submaximal ADP-stimulated respiration is impaired in ZDF rats and recovered by resveratrol. J Physiol. 2013; 591:6089–6101. [PubMed: 24081154]
32. Paglialunga S, Ludzki A, Root-McCaig J, Holloway GP. In adipose tissue, increased mitochondrial emission of reactive oxygen species is important for short-term high-fat diet-induced insulin resistance in mice. Diabetologia. 2015; 58:1071–1080. [PubMed: 25754553]
33. Cannon B, Nedergaard J. Studies of thermogenesis and mitochondrial function in adipose tissues. Methods Mol Biol. 2008; 456:109–121. [PubMed: 18516556]
34. Shabalina IG, Petrovic N, de Jong JM, Kalinovich AV, Cannon B, Nedergaard J. UCP1 in brite/beige adipose tissue mitochondria is functionally thermogenic. Cell Reports. 2013; 5:1196–1203. [PubMed: 24290753]
35. Fisher-Wellman KH, Lin CT, Ryan TE, et al. Pyruvate dehydrogenase complex and nicotinamide nucleotide transhydrogenase constitute an energy-consuming redox circuit. Biochem J. 2015; 467:271–280. [PubMed: 25643703]
36. Brand MD, Nicholls DG. Assessing mitochondrial dysfunction in cells. Biochem J. 2011; 435:297–312. [PubMed: 21726199]
37. Smith BK, Perry CG, Koves TR, et al. Identification of a novel malonyl-CoA IC (50) for CPT-I: implications for predicting in vivo fatty acid oxidation rates. Biochem J. 2012; 448:13–20. [PubMed: 22928974]
38. Dupont J, Mathias MM, Cabacungan NB. Dietary lipid, fatty acid synthesis and cholesterol metabolism in aging rats. Lipids. 1972; 7:576–589. [PubMed: 5084155]
39. Wikström M, Casey R. The oxidation of exogenous cytochrome c by mitochondria. Resolution of a long-standing controversy. FEBS Lett. 1985; 183:293–298. [PubMed: 2985431]
40. Echtay KS, Esteves TC, Pakay JL, et al. A signalling role for 4-hydroxy-2-nonenal in regulation of mitochondrial uncoupling. EMBO J. 2003; 22:4103–4110. [PubMed: 12912909]
41. Nègre-Salvayre A, Hirtz C, Carrera G, et al. A role for uncoupling protein-2 as a regulator of mitochondrial hydrogen peroxide generation. FASEB J. 1997; 11:809–815. [PubMed: 9271366]
42. Zheng J, Ramirez VD. Inhibition of mitochondrial proton F0F1-ATPase/ATP synthase by polyphenolic phytochemicals. Br J Pharmacol. 2000; 130:1115–1123. [PubMed: 10882397]
43. Lambert JE, Ramos-Roman MA, Browning JD, Parks EJ. Increased de novo lipogenesis is a distinct characteristic of individuals with nonalcoholic fatty liver disease. Gastroenterology. 2014; 146:726–735. [PubMed: 24316260]
44. Donnelly KL, Smith CI, Schwarzenberg SJ, Jessurun J, Boldt MD, Parks EJ. Sources of fatty acids stored in liver and secreted via lipoproteins in patients with nonalcoholic fatty liver disease. J Clin Invest. 2005; 115:1343–1351. [PubMed: 15864352]
45. Carling D, Zammit VA, Hardie DG. A common bicyclic protein kinase cascade inactivates the regulatory enzymes of fatty acid and cholesterol biosynthesis. FEBS Lett. 1987; 223:217–222. [PubMed: 2889619]
46. Crane JD, Palanivel R, Mottillo EP, et al. Inhibiting peripheral serotonin synthesis reduces obesity and metabolic dysfunction by promoting brown adipose tissue thermogenesis. Nat Med. 2015; 21:166–172. [PubMed: 25485911]
47. Sidossis L, Kajimura S. Brown and beige fat in humans: thermogenic adipocytes that control energy and glucose homeostasis. J Clin Invest. 2015; 125:478–486. [PubMed: 25642708]
48. Enerbäck S, Jacobsson A, Simpson EM, et al. Mice lacking mitochondrial uncoupling protein are cold-sensitive but not obese. Nature. 1997; 387:90–94.
49. Williamson RT. On the treatment of glycosuria and diabetes mellitus with sodium salicylate. BMJ. 1901; 1:760–762. [PubMed: 20759517]

50. Cameron AR, Logie L, Patel K, et al. Investigation of salicylate hepatic responses in comparison with chemical analogues of the drug. Biochim Biophys Acta. 2016; 1862:1412–1422. [PubMed: 27130437]
51. Ariel D, Kim SH, Liu A, et al. Salsalate-induced changes in lipid, lipoprotein, and apoprotein concentrations in overweight or obese, insulin-resistant, non-diabetic individuals. J Clin Lipidol. 2015; 9:658–663. [PubMed: 26350812]
52. Cao Y, Dubois DC, Sun H, Almon RR, Jusko WJ. Modeling diabetes disease progression and salsalate intervention in Goto-Kakizaki rats. J Pharmacol Exp Ther. 2011; 339:896–904. [PubMed: 21903749]
53. Sproull DH. A peripheral action of sodium salicylate. Br Pharmacol Chemother. 1954; 9:262–264.
54. Haas R, Parker WD Jr, Stumpf D, Eguren LA. Salicylate-induced loose coupling: protonmotive force measurements. Biochem Pharmacol. 1985; 34:900–902. [PubMed: 3977963]
55. Sproull DH. A comparison of sodium salicylate and 2:4-dinitrophenol as metabolic stimulants in vitro. Biochem J. 1957; 66:527–532. [PubMed: 13459891]
56. Denis W, Means JH. The influence of salicylate on metabolism in man. J Pharmacol Exp Ther. 1916; 8:273–283.
57. Hundal RS, Petersen KF, Mayerson AB, et al. Mechanism by which high-dose aspirin improves glucose metabolism in type 2 diabetes. J Clin Invest. 2002; 109:1321–1326. [PubMed: 12021247]
58. Cochran JB. The respiratory effects of salicylate. BMJ. 1952; 2:964–967. [PubMed: 12987706]
59. Brody TM. Action of sodium salicylate and related compounds on tissue metabolism in vitro. J Pharmacol Exp Ther. 1956; 117:39–51. [PubMed: 13320299]
60. Gutknecht J. Salicylates and proton transport through lipid bilayer membranes: a model for salicylate-induced uncoupling and swelling in mitochondria. J Membr Biol. 1990; 115:253–260. [PubMed: 2165171]
61. Gutknecht J. Aspirin, acetaminophen and proton transport through phospholipid bilayers and mitochondrial membranes. Mol Cell Biochem. 1992; 114:3–8. [PubMed: 1334228]
62. Perry RJ, Zhang D, Zhang XM, Boyer JL, Shulman GI. Controlled-release mitochondrial protonophore reverses diabetes and steatohepatitis in rats. Science. 2015; 347:1253–1256. [PubMed: 25721504]
63. Tao H, Zhang Y, Zeng X, Shulman GI, Jin S. Niclosamide ethanolamine-induced mild mitochondrial uncoupling improves diabetic symptoms in mice. Nat Med. 2014; 20:1263–1269. [PubMed: 25282357]
64. Samuel VT, Liu ZX, Qu X, et al. Mechanism of hepatic insulin resistance in non-alcoholic fatty liver disease. J Biol Chem. 2004; 279:32345–32353. [PubMed: 15166226]
65. Figarola JL, Singhal P, Rahbar S, Gugiu BG, Awasthi S, Singhal SS. COH-SR4 reduces body weight, improves glycemic control and prevents hepatic steatosis in high fat diet-induced obese mice. PLoS One. 2013; 8:e83801. [PubMed: 24376752]
66. Kalinovich AV, Shabalina IG. Novel Mitochondrial Cationic Uncoupler C4R1 Is an Effective Treatment for Combating Obesity in Mice. Biochemistry (Mosc). 2015; 80:620–628. [PubMed: 26071782]
67. Smith MJ, Moses V. Uncoupling reagents and metabolism. 1. Effects of salicylate and 2:4-dinitrophenol on the incorporation of C from labelled glucose and acetate into the soluble intermediates of isolated rat tissues. Biochem J. 1960; 76:579–585. [PubMed: 16748836]
68. Keating SE, Hackett DA, Parker HM, et al. Effect of aerobic exercise training dose on liver fat and visceral adiposity. J Hepatol. 2015; 63:174–182. [PubMed: 25863524]
69. Colberg SR, Sigal RJ, Fernhall B, et al. American College of Sports Medicine; American Diabetes Association. Exercise and type 2 diabetes: the American College of Sports Medicine and the American Diabetes Association: joint position statement. Diabetes Care. 2010; 33:e147–e167. [PubMed: 21115758]
70. Stanford KI, Middelbeek RJ, Townsend KL, et al. Brown adipose tissue regulates glucose homeostasis and insulin sensitivity. J Clin Invest. 2013; 123:215–223. [PubMed: 23221344]
71. Blacker TS, Mann ZF, Gale JE, et al. Separating NADH and NADPH fluorescence in live cells and tissues using FLIM. Nat Commun. 2014; 5:3936. [PubMed: 24874098]

72. Harriman G, Greenwood J, Bhat S, et al. Acetyl-CoA carboxylase inhibition by ND-630 reduces hepatic steatosis, improves insulin sensitivity, and modulates dyslipidemia in rats. Proc Natl Acad Sci U S A. 2016; 113:E1796–E1805. [PubMed: 26976583]

73. DeFronzo RA, Gunnarsson R, Björkman O, Olsson M, Wahren J. Effects of insulin on peripheral and splanchnic glucose metabolism in noninsulin-dependent (type II) diabetes mellitus. J Clin Invest. 1985; 76:149–155. [PubMed: 3894418]

74. Fawaz G, Tutunji B. The mechanism of dinitrophenol heart failure. Br Pharmacol Chemother. 1957; 12:273–278.

75. Tainter ML, Cutting WC, Stockton AB. Use of dinitrophenol in nutritional disorders: a critical survey of clinical results. Am J Public Health Nations Health. 1934; 24:1045–1053. [PubMed: 18014064]

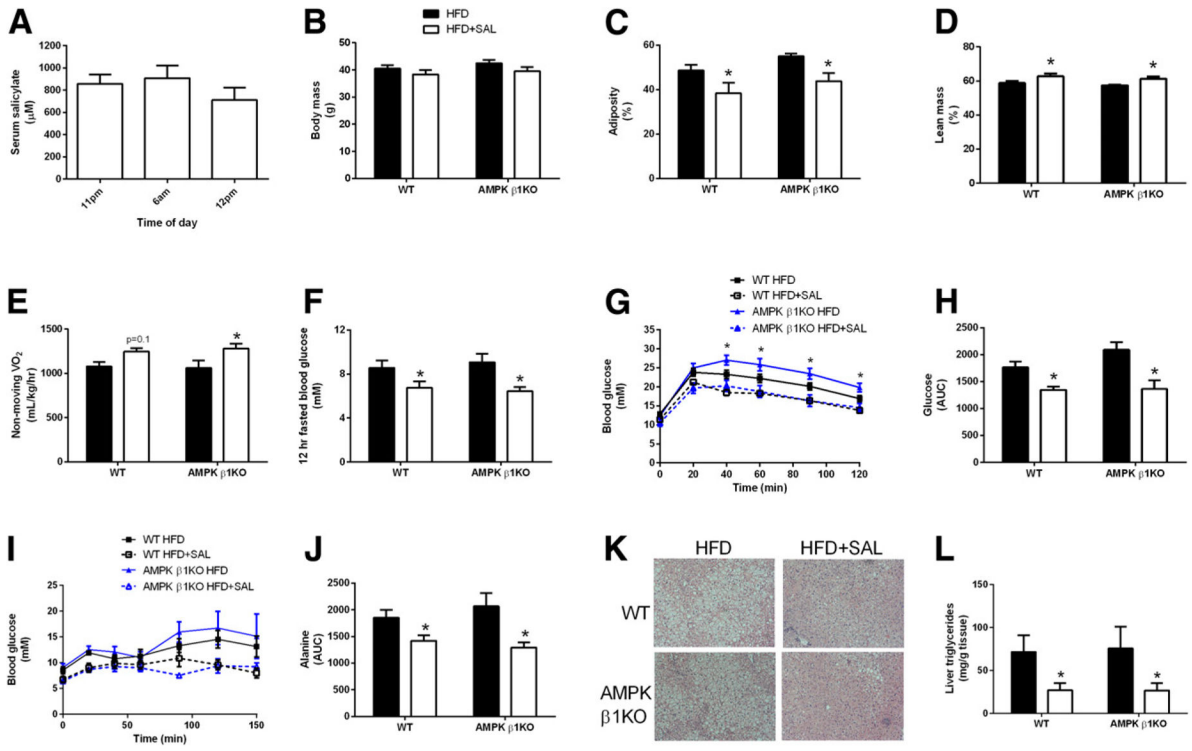

Figure 1.

Salsalate supplementation improves glucose homeostasis and reduces liver lipids independent of AMPK-β1. *A*: Serum salicylate concentrations in mice after treatment with 2.5 g/kg salsalate supplemented into a 60% HFD (HFD+SAL). Body mass (*B*), adiposity (*C*), lean mass (D), nonmoving VO_2 (*E*), and fasting blood glucose (*F*) in WT and AMPK-β1KO mice fed the HFD or HFD+SAL. Glucose tolerance (*G* and *H*) and alanine tolerance (*I* and *J*) in WT and AMPK-β1KO mice fed the HFD or the HFD+SAL. Liver sections were stained with hematoxylin and eosin (*K*), and lipid content was quantified (*L*). AUC, area under the curve. Data are expressed as mean ± SEM (n = 9–17). *$P < 0.05$ by two-way ANOVA with Bonferroni post hoc test.

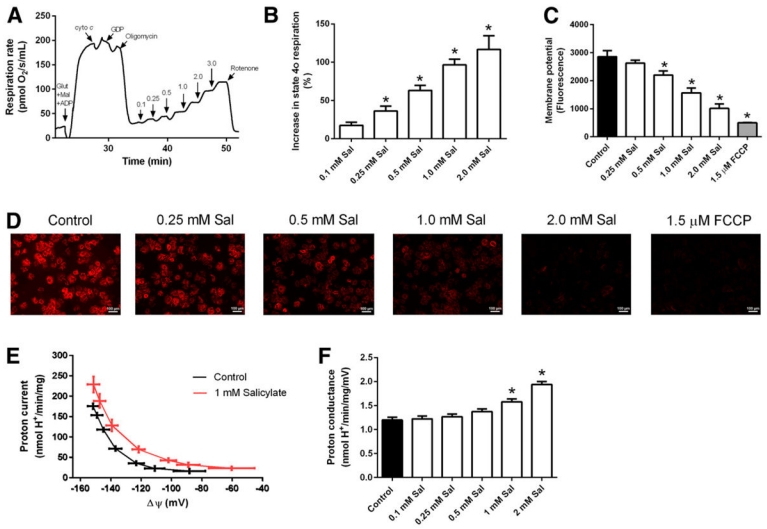

Figure 2.

Salicylate uncouples primary hepatocytes, reduces mitochondrial membrane potential, and increases mitochondrial proton conductance. *A*: Representative oxygraph trace in permeabilized primary hepatocytes illustrates the change in oligomycin-insensitive respiration (state 4o) during salicylate titration. *B*: Quantification of the increase in state 4o respiration when titrating salicylate (Sal). *C* and *D*: Change in TMRM fluorescence in response to salicylate in permeabilized primary hepatocytes. FCCP, carbonyl cyanide-4-(trifluoromethoxy) phenylhydrazone. *E*: Proton current at a given membrane potential in the presence or absence (control) of 1 mmol/L salicylate. *F*: Proton conductance alterations with salicylate titration. Data are expressed as mean ± SEM ($n = 3–6$). *$P < 0.05$ by one-way ANOVA with Bonferroni post hoc test or two-tailed Student *t* test.

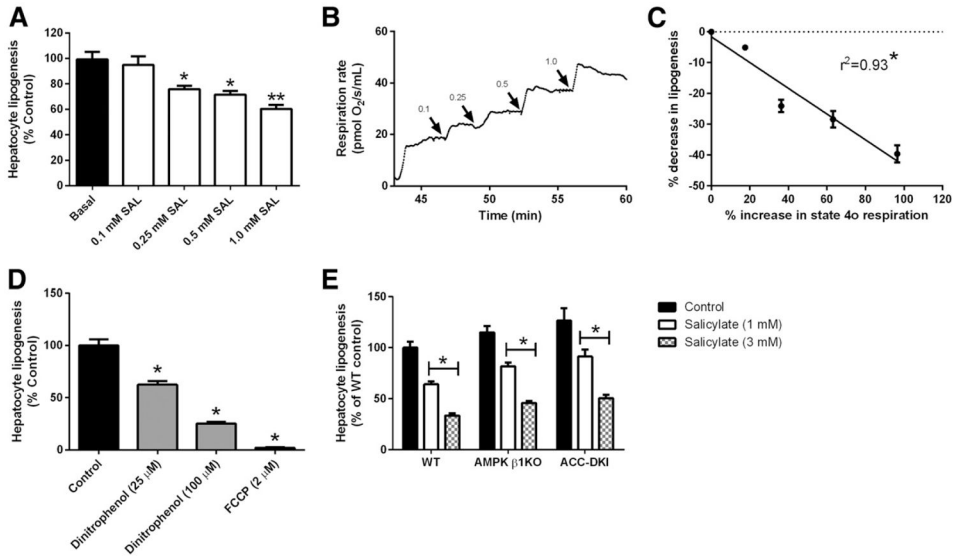

Figure 3.

In vitro, hepatic de novo lipogenesis is inhibited by salicylate. *A*: De novo lipogenesis (from ^{3}H acetate) in primary hepatocytes treated with salicylate (SAL) at subclinical to clinical concentrations. *B*: Representative trace of salicylate-driven mitochondrial uncoupling at subclinical to clinical concentrations. *C*: Correlation between increase in state 4o respiration and reduction in de novo lipogenesis. *D*: The effect of two mitochondrial uncouplers, DNP and carbonyl cyanide-4-(trifluoromethoxy) phenylhydrazone (FCCP), on rates of de novo lipogenesis. *E*: De novo lipogenesis in primary hepatocytes derived from WT, AMPK-β1KO, and ACC-DKI treated with salicylate. Data are expressed as mean ± SEM (n = 4–8). *P < 0.05 and **P < 0.001 by one-way ANOVA with Bonferroni post hoc test was used to detect statistical differences.

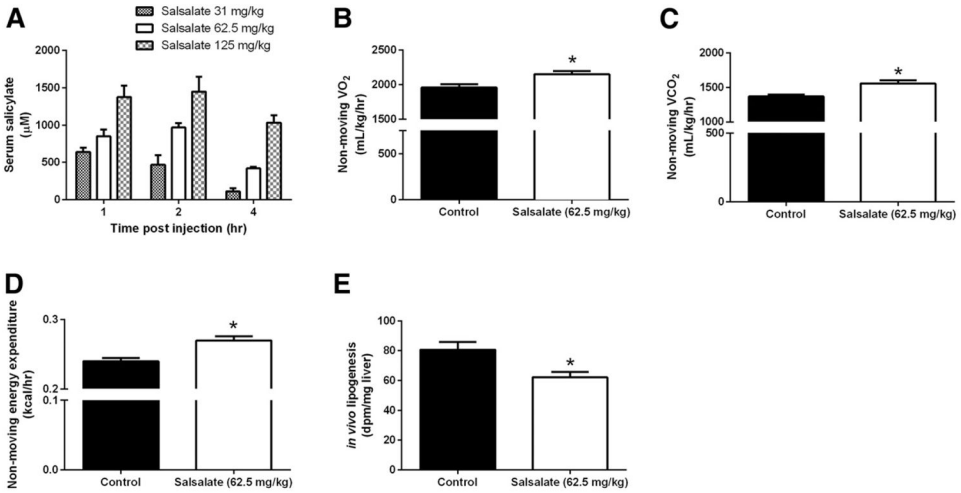

Figure 4.

In vivo, hepatic de novo lipogenesis is inhibited by salsalate. *A*: Circulating salicylate concentrations are shown after three different intraperitoneal injections of salsalate. Nonmoving VO_2 (*B*), nonmoving VCO_2 (*C*), energy expenditure (*E*), and hepatic de novo lipogenesis rates (from ^3H acetate) in response to salsalate injections (62.5 mg/kg i.p.) are shown in WT chow-fed mice. DPM, disintegrations per minute. Data are expressed as mean ± SEM ($n = 4–6$). *$P < 0.05$ by two-tailed Student *t* test.

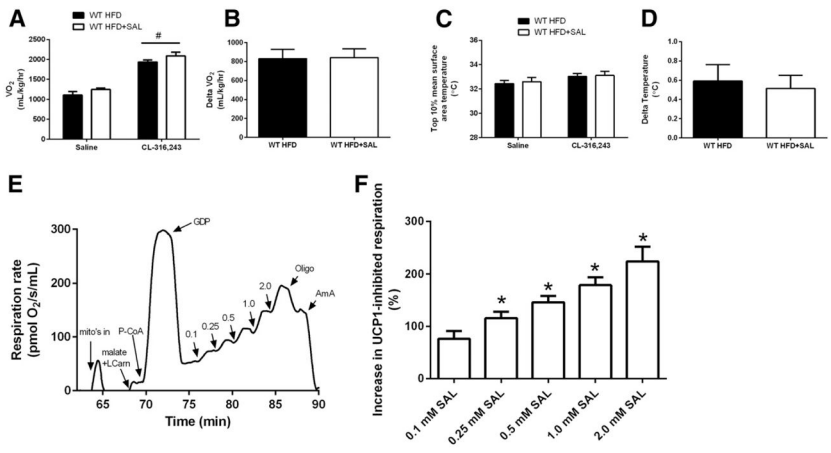

Figure 5.

Salsalate does not alter BAT thermogenesis in vivo, but salicylate increases UCP1-inhibited BAT mitochondrial respiration in vitro. *A* and *B*: VO_2 response to CL-316,243 (0.033 nmol/g body weight) in mice fed the HFD or the HFD with salsalate supplementation (HFD +SAL). *C* and *D*: BAT thermogenesis in response to CL-316,243 in HFD and HFD+SAL mice. *E*: Representative trace of salicylate-driven BAT mitochondrial respiration in the presence of 2 mmol/L GDP. AmA, antimycin A; LCarn, L-carnitine; P-CoA, palmitoyl-CoA. *F*: Quantification of the increase in respiration when titrating salicylate. Data are expressed as mean ± SEM ($n = 5–9$ for in vivo data and $n = 6$ for BAT mitochondrial respiration experiments). #$P < 0.05$ by two-way ANOVA with Bonferroni post hoc test compared with saline and *$P < 0.05$ by one-way ANOVA were used to detect statistical differences.